HIGH RESOLUTION NUCLEAR MAGNETIC RESONANCE STUDIES OF THE CONFORMATION AND ORIENTATION OF MELITTIN BOUND TO A LIPID-WATER INTERFACE

LARRY R. BROWN, WERNER BRAUN, ANIL KUMAR, AND KURT WÜTHRICH
Institut Für Molekularbiologie und Biophysik, Eidgenössische Technische Hochschule, ETH-Hönggerberg, CH-8093 Zürich, Switzerland

ABSTRACT Previously, the size and stoichiometry of mixed micelles of perdeuterated dodecylphosphocholine and melittin were characterized and the ^1H NMR spin systems of most amino acid residues of micelle-bound melittin identified. One- and two-dimensional ^1H-^1H Overhauser experiments have now been used to obtain qualitative information on intramolecular proton-proton distances. These data show that the N-terminal and the C-terminal segments of melittin form two spatially distinct, compact domains; using lipid spin labels these could be located near the micelle surface. For the C-terminal domain a detailed conformation was determined by using the distance contraints from the Overhauser studies as input for a distance geometry algorithm.

INTRODUCTION

Since the introduction of the fluid mosaic model of membrane organization (1), impressive progress has been made in elucidating the topological implications of this model. For both the protein and the lipid components of membranes, considerable information on the distribution and mobility in both transmembrane and lateral directions has been obtained (e.g., 2, 3) and some of the mechanisms involved in establishment and maintenance of membrane topology have been elucidated (e.g., 4). When one turns from these topological characteristics to structural features on the molecular level, present understanding is much less complete. Although general principles of lipid organization have emerged (e.g., 5), information on conformations of membrane-bound polypeptides and proteins is still rather scarce. Furthermore, research into the structural basis of protein-lipid interactions has concentrated almost exclusively on the lipid components (e.g., 5, 6).

From the experience gained with water-soluble proteins, single crystal x-ray studies and high resolution nuclear magnetic resonance (NMR) would be the techniques of choice for obtaining detailed conformational information for polypetide chains associated with lipids. However, fundamental and practical difficulties have so far prevented extensive application to membrane proteins. It appeared therefore of interest to use suitable model systems to obtain detailed, many-parameter information on lipid-bound polypeptides. We have shown that high-resolution ^1H NMR spectra can be obtained for polypeptide chains bound to perdeuterated micellar lipids or detergents (7) and evidence was obtained that similar conformations prevailed for polypeptides bound to such micelles and to lipid bilayers in vesicles (8, 9). Various physicochemical methods have been used to characterize size and stoichiometry of mixed micelles formed from perdeuterated lipid and melittin (8) or glucagon (9). ^1H NMR techniques were developed to outline the global features of the conformations of micelle-bound polypeptide chains (9, 10) and, combined with a suitable distance geometry algorithm for the structural analysis of the spectral data, to determine in detail the spatial structures for distinct segments of the polypeptides (11). Finally, to characterize further the assembly of lipid and polypeptide molecules in the mixed micelles and to investigate the location of the polypeptide relative to the micelle surface, we introduced lipid spin labels into the micelles and measured the electron paramagnetic resonance (EPR) spectra as well as the effects of the spin labels on the NMR spectra (12).

The present paper reports on the conformation of melittin bound to dodecylphosphocholine micelles, which was determined with the techniques mentioned above. The figures and tables present new experimental and theoretical work on the conformation of the C-terminal segment 16–24 of melittin and its orientation relative to the micelle surface. This new data is discussed in the light of previously published results on the global features of the

---

Dr. Kumar is on leave from the Department of Physics, Indian Institute of Science, Bangalore, India.
Dr. Brown's present address is the Michigan Molecular Institute, Midland, Michigan 48640.

conformation of micelle-bound melittin (13) and on the spatial structures of monomeric and tetrameric melittin in aqueous solution (14, 15).

Melittin is a polypeptide of 26 amino acid residues which constitutes ~ 50% of the dry weight of bee venom. Melittin has a variety of effects on natural membranes including lysis (16); activation of exogenous or endogenous phospholipase A (17, 18); alterations in mitochondrial respiration (19) and adenylate cyclase activity (20); and specific changes in coupling of photosynthetic systems (21). These effects of melittin appear to result from the ability of the polypeptide to alter lipid organization (e.g., 22, 23), so that comparative studies of melittin in aqueous solution and in lipid-water interfaces are of particular interest with regard to the structural basis of its biological functions.

MATERIALS AND METHODS

The major, nonformylated component of *Apis mellifera* melittin (14, 16) was used. The synthesis and/or origin of fully deuterated dodecylphosphocholine (7) and the spin labels 5-doxylstearate, 12-doxylstearate, 16-doxylstearate and 1-oxyl-4-dodecylphospho-2,2,6,6-tetramethyl piperidine (12) as well as the preparation of the NMR samples (9, 11) were described previously. The composition of the samples is given in the figure captions.

Fourier transform ^{1}H NMR spectroscopy at 360 MHz, truncated driven nuclear Overhauser enhancement (TOE) difference spectroscopy (24), and two-dimensional (2D) nuclear Overhauser enhancement spectroscopy (NOESY) (25) were performed on a Bruker HX 360 spectrometer (Bruker Instruments, Inc., Billerica, MA) equipped with an Aspect 2000 computer. ^{13}C NMR spectra at 25.1 MHz were recorded on a Varian XL 100 spectrometer (Varian Associates, Inc., Palo Alto, CA).

The distance geometry algorithm used for the structural interpretation of the NOE data, developed on the basis of a similar algorithm by Crippen et al. (26), has recently been described in detail (11). When preparing the input for the computer program from the NOE data we followed the procedures outlined in this earlier paper (11).

RESULTS AND DISCUSSION

Selective ^{1}H-^{1}H Overhauser Effects

With the use of spin echo correlated spectroscopy (SECSY) (27) and a variety of one-dimensional ^{1}H NMR experiments, 96 resonances corresponding to 150 of the 179 nonlabile hydrogens of melittin have been identified and assigned to amino acid types (13). This included identification of the complete spin systems for 17 of the 26 residues of melittin and of portions of the spin systems for eight of the remaining nine residues (13). Only the four spin systems of Gly-1, Ile-2, Ser-18 and Trp-19 were by these experiments assigned to specific positions (13). However, the uneven distribution of most amino acid types in the amino acid sequence of melittin,

Gly-Ile-Gly-Ala-Val-Leu-Lys-Val-Leu-Thr-Thr-Gly-Leu-Pro-
5 10
Ala-Leu-Ile-Ser-Trp-Ile-Lys-Arg-Lys-Arg-Gln-Gln-NH_2,
15 20 25

permitted us to demonstrate, with a recently described application of TOE difference spectroscopy (10), that the amino-terminal and the carboxy-terminal segments of the polypeptide constitute spatially distinct, compact domains in the conformation adopted by micelle-bound melittin (13). To investigate the conformation of the C-terminal domain further, additional selective NOE's between protons of the polypeptide segment 16–24 have been measured (Table I).

TABLE I
NOE CONNECTIVITIES BY DIRECT CROSS-RELAXATION* BETWEEN PROTON RESONANCES OF RESIDUES 16–24 IN MELITTIN BOUND TO PERDEUTERATED DODECYLPHOSPHOCHOLINE MICELLES‡§

δ‡	Assignment	δ‡	Assignment
1.038	Leu-16 δ CH_3	3.692	Ile-17§ αCH
		2.24	Ile-20§ γCH
		7.560	Trp-19 C4H
		6.851	Trp-19 C5H
0.937	Leu-16 δ CH_3	7.560	Trp-19 C4H
4.264	Leu-16§ αCH	7.560	Trp-19 C4H
3.692	Ile-17§ αCH	2.12	Ile-20§ βCH
		0.921	Ile-20§ γCH_3
0.921	Ile-17§ γCH_3	2.94	Lys-II εCH_2
4.206	Ser-18 αCH	2.94	Lys-II εCH_2
4.254	Trp-19 αCH	3.22	Arg-I δCH_2
7.560	Trp-19 C4H	3.327	Ile-20§ αCH
		2.12	Ile-20§ βCH
		2.24	Ile-20§ γCH
		0.60	Lys-I γCH
6.851	Trp-19 C5H	3.327	Ile-20§ αCH
		2.24	Ile-20§ γCH
7.028	Trp-19 C6H	2.742	Lys-I εCH
		2.560	Lys-I εCH
		0.60	Lys-I γCH
7.490	Trp-19 C7H	2.742	Lys-I εCH
		2.560	Lys-I εCH
		0.60	Lys-I γCH
7.372	Trp-19 C2H	0.60	Lys-I γCH
		3.22	Arg-I δCH_2
3.33	Ile-20§ αCH	1.45	Lys-I βCH_2
		0.60	Lys-I γCH
0.921	Ile-20§ γCH_3	3.12	Arg-II δCH_2
		3.86	Lys-II§ αCH
3.86	Lys-II§ αCH	3.12	Arg-II δCH_2

*Obtained from TOE difference spectra recorded with a preirradiation time of 0.4 s^{-1} and/or from a NOESY spectrum recorded with a mixing time of 0.2 s (Figs. 1–3). Listed are those NOE's which were used as input for the distance geometry algorithm. Many of the NOE's listed can be observed in Figs. 2 and 3. Some NOE's, however, were only observed in TOE difference spectra, e.g. the NOE's with Lys I γCH, which were documented previously (Fig. 9 of [13]), do not show up in the contour levels used for Fig. 1 since they give rise to rather broad lines (13).

‡Each row in the table lists the chemical shifts, δ, in ppm relative to internal sodium 3-trimethylsilyl-[2,2,3,3-$^2H_4$]-propionate [TSP] at p^{2}H = 5.5 and T = 37°C and the assignments for two resonance lines between which a NOE was observed. Roman numerals indicate arbitrary notations for spin systems which were not individually assigned (13).

§These resonance assignments to individual residues or to amino acid types were obtained from the interpretation of the NMR data with the distance geometry algorithm (see text).

The data in Table I resulted from two-dimensional NOE spectroscopy (NOESY) (25) and from TOE difference spectra (24). In the NOESY spectrum of Fig. 1, peaks along the diagonal correspond to the normal, one-dimensional spectrum. Pairs of cross peaks in symmetrical locations with respect to the diagonal indicate selective NOE's between diagonal resonance lines. Thus the spectral region ω_1 = 6.5–8.0 ppm, ω_2 = 6.5–8.0 ppm, contains cross peaks corresponding to NOE's between different aromatic protons; the region 0.0–4.5 ppm, 6.5–8.0 ppm contains NOE's between aromatic and aliphatic protons; and the region 0.0–4.5 ppm, 0.0–4.5 ppm contains NOE's between different aliphatic protons. To clarify the analysis of the NOESY spectrum, in Figs. 2 and 3, two regions are shown on an expanded scale and with inclusion of lower contour levels; the cross-peaks are assigned as described in the figure captions. Figs. 2 and 3 contain only a few cross-peaks between resonances which are well resolved along both the ω_1 and ω_2 axes. Therefore many of the assignments given in these two figures were verified with one-dimensional TOE difference spectra recorded with a preirradiation time of 0.4 s with or without selective spin decoupling (29). Mainly because of the possibility of spin

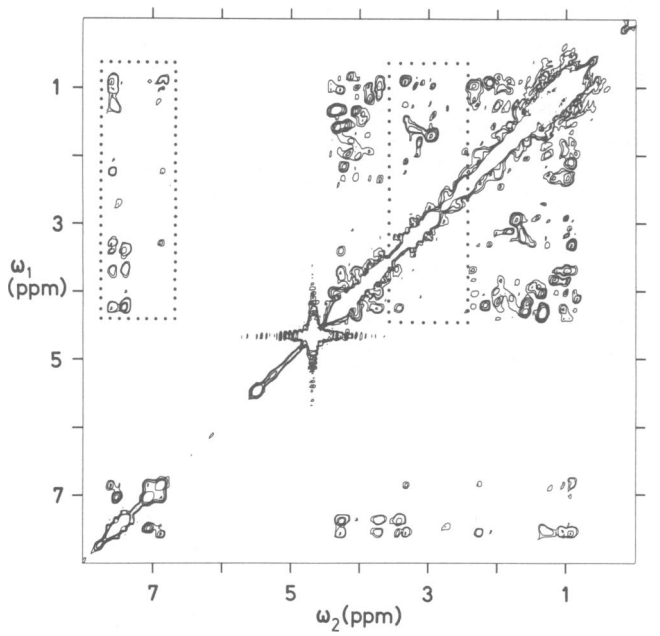

FIGURE 1 Contour plot of a 2D NOE (NOESY) ^{1}H NMR spectrum at 360 MHz recorded for a solution containing $8 \cdot 10^{-3}$ M melittin and 0.36 M [$^2H_{38}$]dodecylphosphocholine at p^{2}H 5.5 and 37°C. The mixing time was 200 ms. The spectral width was 3,500 Hz. The data set consisted of 512 points in both dimensions. Before Fourier transformation the free induction decays were multiplied with a phase-shifted sine bell, sin [$\pi (t+t_0)/t_s$], where t_s is the experimental acquisition time and t_0/t_s was 1/64 (25). After Fourier transformation, the spectrum was further improved by symmetrization. (Symmetrization of 2D NMR spectra is an as yet unpublished technique which is closely related to diagonal multiplication [28].) The two spectral regions enclosed by dotted lines are shown in Figs. 2 and 3 on an expanded scale and with inclusion of lower contour levels.

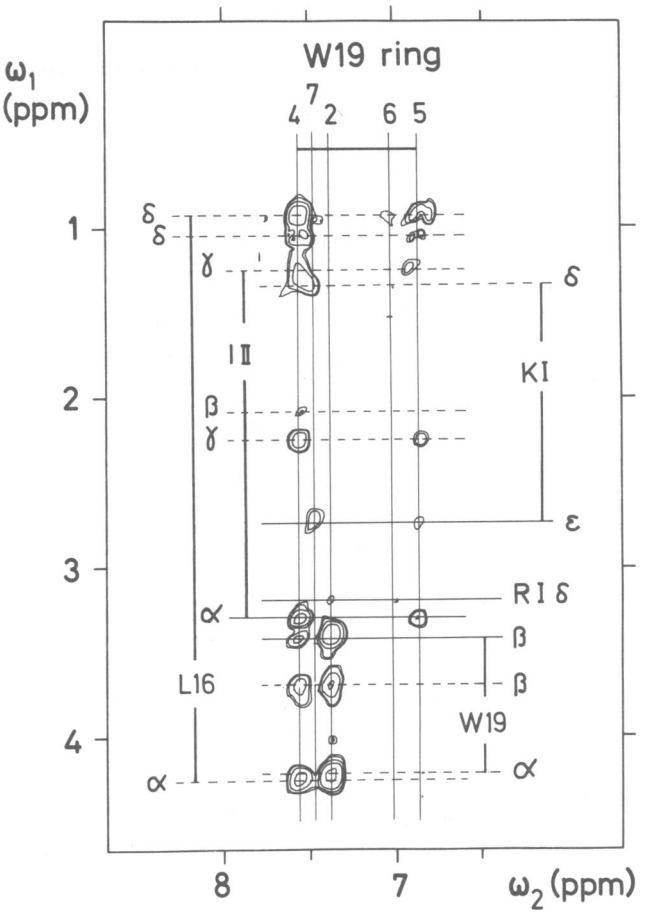

FIGURE 2 Expanded plot of the region ω_1 = 0.5–4.5 ppm, ω_2 = 6.5–8.0 ppm in the NOESY spectrum of Fig. 1. The assignments of the NOE cross-peaks are indicated as follows: Where more than one resonance from the same residues gives rise to NOE's, the group of resonances from the same residue is indicated by the heavy solid lines. Thin solid lines are drawn through the cross-peaks for resonances which are individually resolved in the one-dimensional ^{1}H NMR spectrum of micelle-bound melittin, e.g., the resonances from the indole ring of Trp-19 (7). Thin dashed lines are drawn through the cross-peaks for resonances which are not resolved in the one-dimensional ^{1}H NMR spectrum of micelle-bound melittin, e.g., the αCH of Trp-19. From the two lines which intersect at a given cross-peak, the spatially proximal hydrogen atoms which give rise to the corresponding NOE are identified.

decoupling (29) and in some instances because of the superior signal:noise ratio, TOE difference spectroscopy provided a valuable complementation of NOESY, even though otherwise there is close coincidence between the results of the two experiments (30).

The formation of spatially separated domains by the N-terminal and C-terminal segments of micelle-bound melittin (13) is also manifested in Figs. 1–3. Thus Figs. 2 and 3 contain NOE's amongst the residues Leu-III (6, 9, 13 or 16); Ile-I and Ile-II (17 and 20); Trp-19; Lys-I and Lys-II (7, 21 or 23) and Arg-I and Arg-II (22 and 24), where the roman numerals denote previously identified spin systems which had not been assigned to specific amino acid residues (13). In contrast, no NOE's were observed

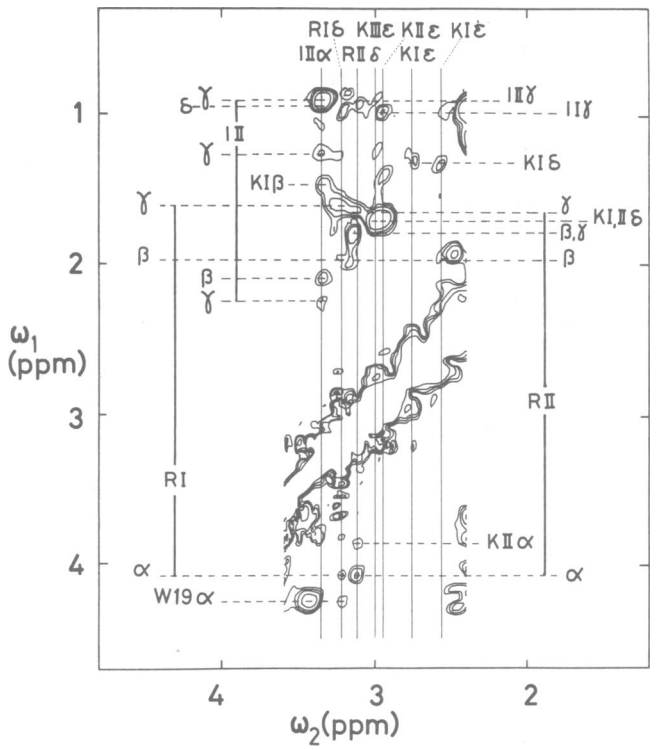

FIGURE 3 Expanded plot of the region ω_1 = 0.5 –4.5 ppm, ω_2 = 2.4–3.6 ppm in the NOESY spectrum of Fig. 1. The assignments of the cross-relaxation peaks are indicated by the scheme described in the caption to Fig. 2.

between these residues and Ile-2, glycines 1, 3 and 12, valines 5 and 8, and threonines 10 and 11. On the basis of the spatial proximity to residues 17, 18, 19, 20, 22, and 24 manifested in the NOE's, the resonances Leu-III were assigned (13) to Leu-16 and the spin systems Lys-I and Lys-II to Lys-21 and Lys-23 (Table I).

Use of a Distance Geometry Algorithm for Individual Assignments and Structural Interpretation of the Overhauser Effects between Protons of Residues 16–24 of Micelle-bound Melittin

If in addition to the distance constraints imposed by the covalent structure all other interatomic distances in a polypeptide chain were known, the corresponding three-dimensional structure could be generated by the presently used distance geometry algorithm (11, 26). For the melittin peptide segment 16–24, however, only a limited number of constraints were obtained from the NOE experiments, and individual assignments were obtained only for some side chain resonances of Leu-16 and the complete spin systems of Ser-18 and Trp-19. For the two isoleucines, two lysines, and two arginines, there are a total of eight possible individual assignments (Table II). To search for those assignments simultaneously compatible with the polypeptide covalent structure, the lower bounds to

TABLE II
POSSIBLE INDIVIDUAL RESONANCE ASSIGNMENTS IN MELITTIN 16–24

Spin System*	Assignments‡							
	A	B	C	D	E	F	G	H
Ile-I	17	17	17	17	20	20	20	20
Ile-II	20	20	20	20	17	17	17	17
Lys-I	23	23	21	21	23	23	21	21
Lys-II	21	21	23	23	21	21	23	23
Arg-I	22	24	22	24	22	24	22	24
Arg-II	24	22	24	22	24	22	24	22

*The Roman numerals I and II denote the previously identified spin systems in the ^{1}H-NMR spectrum (13).
‡Assignments A-H are obtained by permutation of the amino acid positions of the two isoleucines (17 and 20) two lysines (21 and 23) and two arginines (22 and 24).

nonbonding distances imposed by the van der Waals radii of the atoms, and the NOE data (Table I), the distance constraints from Table I were used as input for distance geometry calculations with the different possible assignments of Table II. Based on previous considerations (11), only upper bounds for the proton-proton distances were derived from the NOE data, i.e., in different calculations it was assumed that the distances between NOE-connected protons (Table I) were, respectively, < 5.0Å or < 4.0Å. Qualitatively similar results were obtained with these two interpretations of the NOE's.

In a first application of the distance geometry algorithm, individual assignments were obtained for the α-protons of Leu-16 and Lys-II (21 or 23). For all the other residues in the segment 16–24 the αCH resonances had previously been identified (13). In Figs. 2 and 3 and additional experiments, NOE's were observed between a hitherto unassigned αCH at 4.264 ppm and the side chain of Leu-16 and the indole ring of Trp-19, and between an αCH at 3.86 ppm and hydrogen atoms of Ile-II (17 or 20), Arg-II (22 or 24) and Lys-II (21 or 23). The assignments of the αCH lines in Table I resulted from evaluation of the NOE data in light of the three-dimensional structures for melittin 16–24 calculated for the eight individual assignments in Table II with all the NOE's in Table I except those involving αCH of Leu-16 or αCH of Lys-II. For all eight assignments it was found that while Leu-16 had numerous contacts to the indole ring of Trp-19 and to Ile-II (17 or 20), there were no close contacts to Arg-II (22 or 24) or to Lys-II (21 or 23). Similarly, Lys-II (21 or 23) showed numerous contacts to Ile-II (17 or 20) and Arg-II (22 or 24), but no contacts to the indole ring of Trp-19 or to Leu-16. Furthermore, with the assignments in Table I, the αCH resonances at 4.264 ppm and 3.86 ppm each show intraresidue NOE's, which was a feature observed throughout the sequence of micelle-bound melittin (13).

The distance-geometry algorithm was then used with the complete set of NOE constraints in Table I to calculate

TABLE III
RESIDUAL VIOLATIONS OF DISTANCE BOUNDS FOR THE EIGHT POSSIBLE INDIVIDUAL RESONANCE ASSIGNMENTS IN MELITTIN 16–24 (TABLE II)

Upper bounds: 4 Å*				Upper bounds: 5 Å*			
Assignment‡	E§	EV‖	NV¶	Assignment‡	E§	EV‖	NV¶
A	0.53	0.0	0	A	0.09	0.0	0
B	1.34	0.48	3	B	0.15	0.0	0
C	2.00	1.48	9	C	0.43	0.27	2
D	1.35	1.12	8	D	0.09	0.0	0
E	20.0	15.5	88	E	1.19	0.88	6
F	27.1	19.3	104	F	2.12	2.11	16
G	34.6	24.8	118	G	4.52	4.60	31
H	23.6	13.8	74	H	2.94	2.66	18

*In the distance geometry calculations it was assumed that observation of a NOE between two groups of protons (Table I) indicated that the proton-proton distance was smaller than 4.0Å, or smaller than 5.0Å, respectively.
‡The letters A to H refer to the resonance assignments in Table II.
§E is the value of the quadratic error function defined in Eqs. 41–43 of reference 11 after 5 G-cycles and 500 refinement cycles.
‖EV (Å) is the sum of the absolute values of all violations of distance bounds ≥0.1Å.
¶NV is the number of distance-bounds violations ≥ 0.1Å.

spatial structures for all eight individual assignments in Table II. Compatibility of these conformations with the covalent structure and the NOE data was judged from the values of the error function E, the number of distance violations exceeding 0.1Å, NV, and the sum of the absolute values of these distance violations, EV (Table III) (11). Table III shows that the assignments A–D, with Ile-I and Ile-II corresponding to Ile-17 and Ile-20, give better compatibility than E–H. That the differences of E, NV and EV between the assignments A–D and E–H (Table III) are significant is clearly demonstrated by Table IV, which lists the corresponding parameters for five different runs with assignment A. Independent of whether the observation of a NOE was taken to indicate an upper bound for the distance between two protons of 4.0Å or 5.0Å (11), clear-cut evidence for the assignments of Ile-17 and Ile-20 was thus obtained. However, the experimental data of Table I are not sufficient to obtain by this method individual assignments for the two lysines and the two arginines in melittin 16–24.

TABLE IV
RESIDUAL VIOLATIONS OF DISTANCE BOUNDS FOR TEN STRUCTURES OF MELITTIN 16–24 CALCULATED WITH THE RESONANCE ASSIGNMENTS A (TABLE II)

Upper bounds: 4 Å*				Upper bounds: 5 Å*			
RUN	E*	EV*	NV*	RUN	E*	EV*	NV*
1	0.54	0.0	0	1′	0.28	0.0	0
2	0.41	0.0	0	2′	0.21	0.0	0
3	0.52	0.1	1	3′	0.08	0.0	0
4	0.53	0.0	0	4′	0.26	0.0	0
5	0.53	0.0	0	5′	0.09	0.0	0

*In the distance geometry calculations it was assumed that observation of a NOE between two groups of protons (Table I) indicated that the proton-proton distance was smaller than 4.0Å, or smaller than 5.0Å, respectively. E, EV and NV are defined in the footnotes to Table III.

As was discussed in detail elsewhere (11), the three-dimensional structures obtained from distance geometry calculations with bounds on proton-proton distances determined by NOE's correspond to individual species in the ensemble of molecular conformations that are compatible with the experiments. Common structural features for this ensemble of molecular conformations can therefore be delineated by inspection of a group of structures obtained in different computer runs from the same data set. Fig. 4 shows such a group of structures, calculated from the NOE data of Table I with the assumptions that the distances between NOE-connected protons were < 4.0Å and that the resonance assignments A (Table II) prevailed. The principal common features of the structures a–d in Fig. 4 are two successive, irregular right-handed turns formed, respectively, by the backbone atoms of residues 16–20 and 20–24. The four structures resulted from runs one to four in Table IV. Table V shows that the root mean square distances between the different structures are of the order of 1.0 Å. Similar right-handed turns

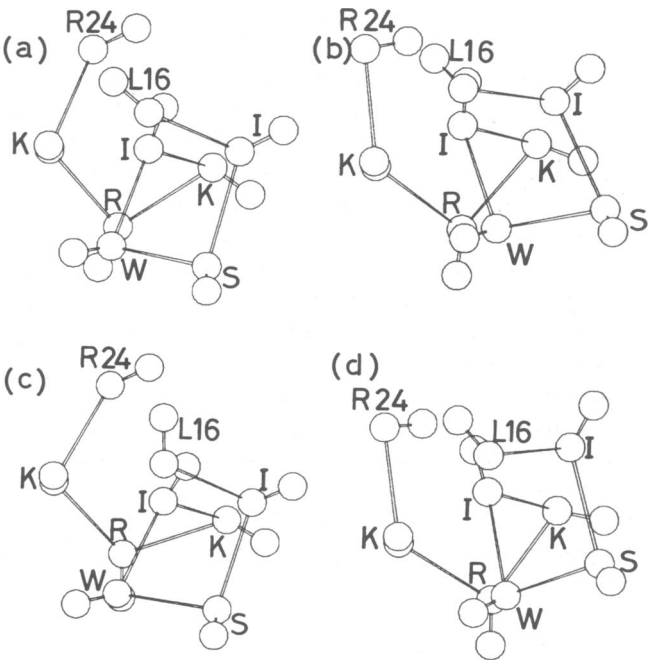

FIGURE 4 Computer drawing of the four structures for micelle-bound melittin 16–24 which were obtained from the computer runs one to four in Table IV. Root mean square distances between these structures are given in Table V. Only the positions of the α- and β-carbon atoms are shown. All four structures were oriented in the same way: First, L 16, I 20 and K 21 were placed in a horizontal plane and then, to avoid overlapping of too many atoms, the structures were rotated by 10° about the horizontal axis through the centroid.

TABLE V
ROOT MEAN SQUARE DISTANCES* BETWEEN FIVE STRUCTURES FOR MELITTIN 16–24 CALCULATED FROM THE DATA IN TABLE I FOR THE RESONANCE ASSIGNMENTS A (TABLE II)

RUN§	1	2	3	4	5
1	—	1.1	1.2	1.0	1.0
2		—	1.3	1.2	1.2
3			—	1.0	1.2
4				—	1.0
5					—

*To quantify the differences between two conformations U and V of a molecule with N atoms, conformation U was first translated relative to V so that the centers of mass coincide, and then rotated so that the sum of the squared distances between corresponding atoms was minimized. The minimal value of

$$\mathrm{RMSD} = \left\{\frac{1}{N}\sum_{j=1}^{N} |R\mathrm{x}_j^U - \mathrm{x}_j^V|^2\right\}^{1/2},$$

obtained with the best fitting rotation matrix, R, called the "root mean square distance between structures U and V." The rotation matrix R which corresponds to the minimum RMSD was obtained using an algorithm proposed by McLachlan (30).
§Correspond to runs 1–5 in Table IV. Runs 1–4 correspond to Fig. 4 *a–d*.

can also be seen in the structures *a*1 and *a*2 of Fig. 5, which resulted from additional computer runs with the same experimental data and resonance assignments *A* (Table II).

Since the two lysines and two arginines in melittin 16–24 were not individually assigned, conformations calculated with the data of Table I for the different assignments *A–D* (Table II) were inspected for common features (Fig. 5). In all eight conformations of Fig. 5 the backbone of residues 16–20 forms a right-handed turn similar to that in the structures of Fig. 4. Although the conformation in the region of residues 21–24 varies considerably with the different individual assignments *A–D* (Table II) of the lysine and arginine spin systems (Fig. 5), a common pattern was observed for the spatial distribution of the positive charges on the arginine and lysine side chains (Fig. 6): all four positive charges lie roughly in a plane which makes an angle of ~ 60°–90°, with the axis of the right-handed turn formed by residues 16–20. The charges are distributed radially relative to the axis of this turn.

Use of Paramagnetic Spin Labels to Determine the Location and Orientation of Micelle-bound Melittin Relative to the Micelle Surface

Small amounts of the spin labels 5-doxylstearate, 12-doxylstearate, 16-doxylstearate and 1-oxyl-4-dodecylphospho-2,2,6,6-tetramethylpiperidine were added to the mixed melittin-dodecylphosphocholine micelles. Previously described (12) control experiments showed that the assembly of lipid and polypeptide molecules in the micelles was not measurably perturbed by the addition of these spin labels, that the nitroxide moieties of 12-doxylstearate and 16-doxylstearate were near the center of the dodecylphosphocholine micelles, and that the nitroxide moieties of 5-doxylstearate and 1-oxyl-4-dodecylphospho-2,2,6,6-tetramethylpiperidine were close to the micelle surface, i.e., at about the level of the detergent phosphate group. On this basis, line broadening of melittin resonances by the different spin labels was used to locate different portions of the melittin amino acid sequence relative to the micelle surface. These data are presented in Table VI and the structural analysis explained in the footnotes to the table.

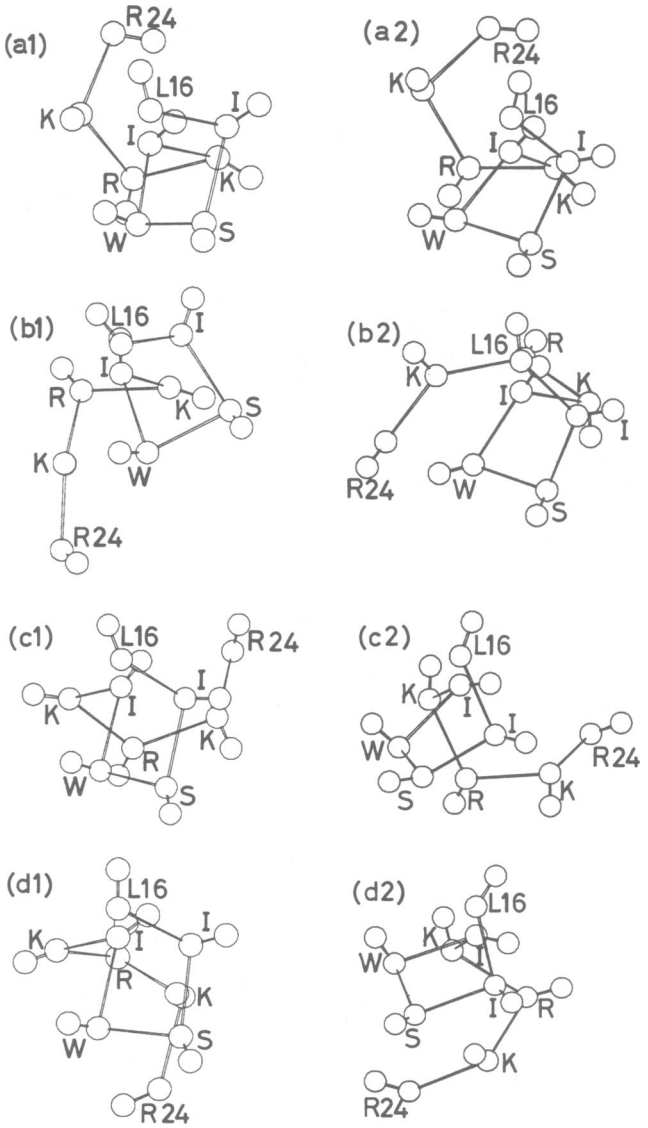

FIGURE 5 Computer drawing of eight structures for micelle-bound melittin 16–24 which were obtained from the computer runs *A–D* in Table III with upper bounds of 4.0Å (*a*1–*d*1) or 5.0Å (*a*2–*d*2). Only the positions of the α- and β-carbon atoms are shown. The molecules are presented in the same orientation as in Fig. 4.

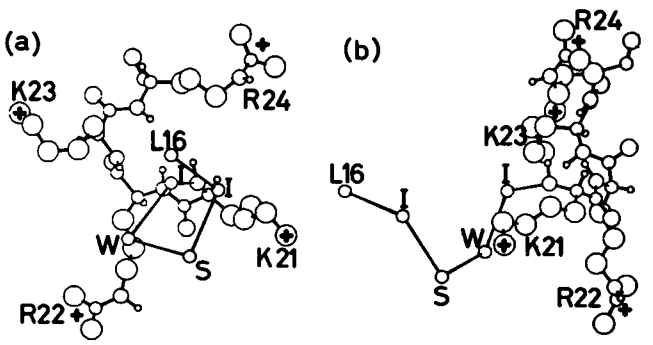

FIGURE 6 Computer drawings of the structure for micelle-bound melittin 16–24 which resulted from the computation 5′ in Table IV, i.e., using assignment *A* (Table II) and upper bounds of 5.0Å. For L 16, I 17, S 18, W 19, and I 20 only the α-carbon atoms are shown. For K 21, R 22, K 23, and R 24 all the atoms are shown, except that, as for the calculations, the CH_2 and NH_2 groups are substituted by "pseudoatoms." The locations of the positive charges are indicated by plus signs. Presentation *a* corresponds to that used for the structures in Fig. 4; presentation *b* was obtained by a 90° counterclockwise rotation about the vertical axis through the center of mass.

With the residues 4, 5, 7, 8, 10, 11, 15, and 19–26 relatively close to the micelle surface and the lack of evidence locating other residues further into the micelle interior (Table VI), and further considering that the apolar interior of dodecylphosphocholine micelles has a thickness of ~ 25Å (8), it is unlikely that melittin penetrates through the micelle interior. Rather, it appears that extended portions of the N-terminal as well as the C-terminal domain of the melittin conformation (13) are near the micelle surface. This conclusion from the spin label data coincides with pH titration data which indicated that the amino groups of Gly-1 and of lysines 7, 21, and 23 were all at the micelle surface (13). A more specific location and orientation can be given for residues 16–24 of micelle-bound melittin. The paramagnetic line-broadening effects indicate that the peripheral side chain protons of residues 21–24 are approximately equidistant from the center of the micelle and near the level of the phosphate group of the detergent molecules in the dodecylphosphocholine micelles (Table VI). From the calculated conformations (Fig. 6), it then appears that the axis of the turn formed by residues 16–20 must lie roughly perpendicular to the micelle surface, with the backbone of residues 16–20 directed towards the micelle interior. The residues 16–20 would thus penetrate 6–8Å into the apolar interior of the micelle. Because evidence was obtained that both the C-terminal and the N-terminal domains of melittin are near the micelle surface, the central region -Thr-10-Thr-11-Gly-12-Leu-13-Pro-14- must form a turn in the apolar micelle interior, causing a reversal of the backbone direction. In an extended form of the peptide segment melittin 10–14 the backbone and the side chains contain numerous polar groups, so that such an orientation of lipid-bound melittin might conceivably result in sufficiently extensive perturbations of lipid bilayer structures to contribute significantly to the physiological effects of this polypeptide mentioned in the Introduction (16–23). Comparing the present experimental data with recently suggested arrangements of melittin bound to lipid aggregates, it appears that they would be compatible with the model by Dawson et al. (32), which explains perturbations of lipid layers by a "wedge effect." On the other hand the present data appear to exclude the "penetration model" proposed by Lavialle et al. (33).

TABLE VI
PARAMAGNETIC LINE-BROADENING FOR ^1H NMR LINES OF MELITTIN BOUND TO SPIN-LABELED DEUTERATED DODECYLPHOSPHOCHOLINE MICELLES*

Amino acid residue	Line-broadening effects for individual resonances			
	Category I‡	Category II‡	Category III‡	Category IV‡
Ala-I (4 or 15)		βCH_3		
Ala-II (4 or 15)		βCH_3		
Lys-7	ϵCH_2			
Val-I (5 or 8)			γCH_3	
Val-II (5 or 8)		γCH_3		
Thr-I (10 or 11)			γCH_3	
Thr-II (10 or 11)			γCH_3	
Trp-19		ring		
Ile-20		αCH		
Lys-I (21 or 23)		ϵCH_2		
Lys-II (21 or 23)		ϵCH_2		
Arg-I (22 or 24)		δCH_2		
Arg-II (22 or 24)		δCH_2		
Gln-I and -II (25 and 26)§	γCH_2			

*The measurements were made in D_2O solutions containing $3 \cdot 10^{-3}$ M melittin, 0.14 M [$^2H_{38}$]dodecylphosphocholine and $5 \cdot 10^{-4}$ M spin label at p^{2}H 5.5 and 50°C.

‡From a detailed analysis of spin label-induced line broadening in glucagon-containing dodecylphosphocholine micelles (12) protons of category I, which show little broadening for all spin labels, are at the surface of or exterior to the micelle; Category II, which shows greatest broadening for 5-doxylstearate and 1-oxyl-4-dodecylphospho-2,2,6,6-tetramethylpiperidine, corresponds to positions at or slightly exterior to the phosphate group of the detergent molecules; Category III, with roughly equal broadening for all spin labels, corresponds to positions slightly interior to the phosphate groups; Category IV, which shows greatest broadening for 12-doxylstearate and 16-doxylstearate, corresponds to positions in the hydrophobic interior of the micelle.

§The γCH_2 resonances of Gln-I and Gln-II were overlapped in the ^1H NMR spectrum (13).

Financial support by the Swiss National Foundation (project number 3.528.79) and use of the facilities of the Zentrum für Interaktives Rechnen (ZIR) of the Eidgenössische Technische Hochschule is gratefully acknowledged.

Received for publication 13 April 1981.

REFERENCES

1. Singer, S. J., and G. R. Nicolson. 1972. The fluid mosaic model of the structure of cell membranes. *Science (Wash., D. C.).* 175:720–731.
2. Shinitzky, M., and P. Henkart. 1979. Fluidity of cell membranes-current concepts and trends. *Int. Rev. Cytol.* 60:121–147.
3. Cherry, R. J. 1979. Rotational and lateral diffusion of membrane proteins. *Biochim. Biophys. Acta.* 559:289–327.
4. Wickner, W. 1979. The assembly of proteins into biological membranes: the membrane trigger hypothesis. *Ann. Rev. Biochem.* 48:23–45.
5. Seelig, J., and A. Seelig. 1980. Lipid conformation in model membranes and biological membranes. *Q. Rev. Biophys.* 13:19–61.
6. Chapman, D., J. C. Gómez-Fernández, and F. M. Goni. 1979. Intrinsic protein-lipid interactions. *Fed. Eur. Biochem. Soc. Lett.* 98:211–223.
7. Brown, L. R. 1979. Use of fully deuterated micelles for conformational studies of membrane proteins by high resolution ^{1}H nuclear magnetic resonance. *Biochim. Biophys. Acta.* 557:135–148.
8. Lauterwein, J., C. Bösch, L. R. Brown, and K. Wüthrich. 1979. Physicochemical studies of the protein-lipid interactions in melittin-containing micelles. *Biochim. Biophys. Acta.* 556:244–264.
9. Bösch, C., L. R. Brown, and K. Wüthrich. 1980. Physicochemical characterization of glucagon-containing lipid micelles. *Biochim. Biophys. Acta.* 603:298–312.
10. Wüthrich, K., C. Bösch, and L. R. Brown. 1980. Conformational studies of lipid-bound polypeptides by elucidation of proton-proton cross-relaxation networks. *Biochem. Biophys. Res. Commun.* 95:1504–1509.
11. Braun, W., C. Bösch, L. R. Brown, N. Gō, and K. Wüthrich. 1981. Combined use of proton-proton Overhauser enhancements and a distance geometry algorithm for determination of polypeptide conformations. *Biochim. Biophys. Acta.* 667:337–396.
12. Brown, L. R., C. Bösch, and K. Wüthrich. 1981. Location and orientation relative to the micelle surface for glucagon in mixed micelles with dodecylphosphocholine: EPR and NMR studies. *Biochim. Biophys. Acta.* 642:296–312.
13. Brown, L. R., and K. Wüthrich. 1981. Melittin bound to dodecylphosphocholine micelles: ^{1}H NMR assignments and global conformational features. *Biochim. Biophys. Acta.* 647:95–111.
14. Lauterwein, J., L. R. Brown, and K. Wüthrich. 1980. High-resolution ^{1}H-NMR studies of monomeric melittin in aqueous solution. *Biochim. Biophys. Acta.* 622:219–230.
15. Brown, L. R., J. Lauterwein, and K. Wüthrich. 1980. High-resolution ^{1}H-NMR studies of self aggregation of melittin in aqueous solution. *Biochim. Biophys. Acta.* 622:231–244.
16. Habermann, E. 1972. Bee and wasp venoms. *Science (Wash., D. C.).* 177:314–322.
17. Mollay, C., G. Kreil, and H. Berger. 1976. Action of phospholipases on the cytoplasmic membrane of *Escherichia coli*. Stimulation by melittin. *Biochim. Biophys. Acta.* 426:317–324
18. Yunes, R., A. R. Goldhammer, W. K. Garner, and E. H. Cordes. 1977. Phospholipases: melittin facilitation of bee venom phospholipase A_2-catalyzed hydrolysis of unsonicated lecithin liposomes. *Arch. Biochem. Biophys.* 183:105–112.
19. Olson, F. C., D. Munjal, and A. N. Malviya. 1974. Structural and respiratory effects of melittin (*Apis mellifera*) on rat liver mitochondria. *Toxicon.* 12:419–425.
20. Lad, P. L., and W. T. Shier. 1980. Effect of melittin-induced membrane alterations on rat heart adenylate cyclase activity. *Arch. Biochem. Biophys.* 204:418–424.
21. Berg, S. P., G. E. Davies, and A. M. Haller. 1980. Electron acceptance at photosystem II in uncoupled spinach thylakoids. *Fed. Eur. Biochem. Soc. Lett.* 117:143–148.
22. Williams, J. C., and Bell, R. M. 1972. Membrane matrix disruption by melittin. *Biochim. Biophys. Acta.* 288:255–262.
23. De Bony, J., J. Dufourcq, and B. Blin. 1979. Lipid-protein interactions: NMR study of melittin and its binding to lysophosphatidycholine. *Biochim. Biophys. Acta.* 552:531–534.
24. Wagner, G., and K. Wüthrich. 1979. Truncated driven nuclear Overhauser effect (TOE). A new technique for studies of selective ^{1}H-^{1}H Overhauser effects in the presence of spin diffusion. *J. Magn. Resonance.* 33:675–680.
25. Anil Kumar, R. R. Ernst, and K. Wüthrich. 1980. A two-dimensional nuclear Overhauser enhancement (2D NOE) experiment for the elucidation of complete proton-proton cross-relaxation networks in biological macromolecules. *Biochem. Biophys. Res. Commun.* 95:1–6.
26. Crippen, G. M., and T. Havel. 1978. Stable calculation of coordinates from distance information. *Acta Crystallogr., Sect. A.* 34:282–284.
27. Nagayama, K., K. Wüthrich, and R. R. Ernst. 1979. Two-dimensional spin echo correlated spectroscopy (SECSY) for ^{1}H NMR studies of biological macromolecules. *Biochem. Biophys. Res. Commun.* 90:305–311.
28. Baumann, R., Anil Kumar, R. R. Ernst, and K. Wüthrich. 1981. Improvement of 2D NOE and 2D correlated spectra by triangular multiplication. *J. Magn. Reson.* 44:76–83.
29. Richarz, R., and K. Wüthrich. 1978. NOE difference spectroscopy: a novel method for observing individual multiplets in proton NMR spectra of biological macromolecules. *J. Magn. Reson.* 30:147–150.
30. Bösch, C., Anil Kumar, R. Baumann, R. R. Ernst and K. Wüthrich. 1981. Comparison of selective proton-proton Overhauser effects in biological macromolecules observed by one-dimensional and two-dimensional NMR experiments. *J. Magn. Reson.* 42:159–163.
31. McLachlan, A. D. 1979. Gene duplications in the structural evolution of chymotrypsin. *J. Mol. Biol.* 128:49–79.
32. Dawson, C. R., A. F. Drake, J. Helliwell, and R. C. Hider. 1978. The interaction of bee melittin with lipid bilayer membranes. *Biochim. Biophys. Acta.* 510:75–86.
33. Lavialle, F., I. W. Levin, and C. Mollay. 1980. Interaction of melittin with dimyristoyl-phosphatidylcholine liposomes. Evidence for boundary lipid by Raman spectroscopy. *Biochim. Biophys. Acta.* 600:62–71.

DISCUSSION

Session Chairman: John N. Weinstein *Scribe*: Heather D. Dettman

SYKES: What are your ideas on the following possible problems with your method of determining a unique final structure? The first is that the distances obtained are the sixth root of the ensemble average of the r^6 values which has the problem that in a flexible structure, it would unfairly weight a small percentage of close contacts. A second concern is the circularity in your approach in that you use four assigned resonances to obtain a structure. You use this structure to assign further resonances then reapply your algorithm to obtain a more refined structure. What are your feelings on the uniqueness of your final structure? Have you checked your results by, for instance, predicting an NOE and noting whether it is present or not?

L. BROWN: I will answer the second question first as it determines whether we are able to treat the two domains, the N-terminal and C-terminal regions, separately for the purpose of calculating structures. We have information as to how many resonances must correspond to the amino-terminal end of the molecule and how many resonances must correspond to the carboxyl-terminal end of the molecule. If you look at the distribution of amino acid residues in melittin, there are distinguishing residues in each end. For example, all of the valines, glycines, and threonines are in the amino-terminal half of the amino acid sequence; two argines, the serine, the tryptophan, and the two glutamines are in the carboxyl-terminal half of the molecule. In the amino-terminal half, there are 85 hydrogen atoms. There are 26 resonances corresponding to 42 hydrogen atoms, that is, 50% of the hydrogen atoms, which we can unambiguously be sure are in the amino terminal region.

It is much the same situation for the carboxyl-terminal region. There are 94 hydrogen atoms. We can identify 39 resonances corresponding to 55 hydrogen atoms which unambiguously correspond to the carboxyl-terminal half of the amino acid sequence. The argument is that we do not see any NOE's between those two groups. This statement may be dangerous if there are only a few resonances which are being considered. However, we observe a large proportion of the hydrogen atoms in each end of the molecule and we know that every residue except proline-14, which was not assigned, shows negative NOE. In this case, it is safe to conclude that the amino-terminal and carboxyl-terminal portions of the sequence are separate spatial domains. This conclusion was actually reached in a previous paper (Brown and Wüthrich, 1981. *Biochim. Biophys. Acta.* 47:95–111) and is discussed in more detail there. We have done not only this two-dimensional NOE experiment, in which the cross-relaxation time is quite short and we should only be seeing nearest neighbors without spin diffusion effects, but have also done experiments under conditions in which spin diffusion, if it were to occur, would be strong. Even here, we do not see any NOE's between the two halves of the molecule.

Your first question actually pertains to the distance geometry alogrithm. How can we take the spectral information and turn it into conformational information? It is important to say why we are worried about flexibility. There is considerable evidence that in both proteins and peptides (and a peptide bound to a micelle is no exception) there is a significant amount of internal flexibility. That means that whatever NMR parameter is measured is an average parameter. Therefore, in using NOE data to obtain molecular conformations, effects of temporal averaging on the experimental parameters must be taken into account. I emphasize that we have not attempted to measure exact or even average interatomic distances, but have instead estimated the largest interatomic distance which would lead to observable NOE under our experimental conditions, including the effects of temporal averaging (reference 11). To ensure that the conformations obtained with the distance-geometry algorithm are physically meaningful, these upper-bound distances are chosen very conservatively. Provided that the upper-bound distances are physically realistic, the conformations obtained with the algorithm are *not* average structures, but are simply different structures which are simultaneously consistent with the covalent structure and the experimental data. The major advantage of using the distance-geometry (reference 11) algorithm is that three-dimensional conformations can be calculated even with only a semi-quantitative interpretation of the experimental data.

In discussing the validity of the structures obtained by the present procedures, it is important to distinguish between the characteristics of the distance-geometry algorithm *per se* and the results obtained with a particular set of experimental data. If exact interatomic distances are known, the distance-geometry algorithm can reconstruct a three-dimensional conformation. For a molecule containing n atoms, this involves determination of 3 n coordinates. However, the $n \times n$ distance matrix contains $(n^2-n)/2$ interatomic distances, which means that this matrix is highly redundant. One of the very attractive features of the distance-geometry algorithm is that because of this redundancy, 3-D conformations can still be determined even when the individual interatomic distances are known only approximately, e.g., as upper and lower bounds on interatomic distances. A striking example of this has been presented by Havel et al. (1980. *Biopolymers.* 18:73–81). For the residues of bovine pancreatic trypsin inhibitor or of carp myogen, they showed that the 3-D conformation observed in the crystal structure could be reconstructed by the distance-geometry algorithm, with a RMS distance deviation of 1 Å or less, simply from a list of whether the residues were or were not within 10 Å of one another. Thus, provided that a sufficient number of constraints are available, the distance-geometry algorithm can use simple yes-no criteria to calculate three-dimensional conformations.

GIERASCH: An individual NOE between two protons does not give any information on distances unless you know the proportion of relaxation that takes place through that proton. It would be necessary to do a triangulation of some sort. How is that built into your algorithm?

L. BROWN: It is important to point out that the 2-D NOE experiment is measuring transient Overhauser effects between two individual resonances. At least for short mixing periods, the intensity of the off-diagonal peak in the 2-D NOE spectrum is directly proportional to the cross-relaxation rate between the two individual resonances (Braun et al. 1981. *Biochim. Biophys. Acta.* 667:337–396.). As you know, the magnitude of the cross-relaxation includes a frequency-dependent term. We can put a limit on the frequency-dependent term. We know that we are working in the negative NOE range. If there is internal motion, the magnitude of the negative NOE should be smaller than if we have a rigid body. This can be used to assign an upper limit to both the frequency and $1/r^6$ terms (Braun et al., 1981).

DEGRADO: I feel that you have done an admirable job of fully defining the chemical and physical properties of the various components you are studying before making your physical measurements. You have demonstrated that rigorous definition of the system which one is studying is essential if meaningful structural information on polypeptides is to be obtained. Nevertheless, I can't help wondering about the relevance of the structures you see at a micelle-water interface to the structure of the same substance on planar phospholipid surfaces. Would you like to comment on this?

L. BROWN: Yes. We are very much in the same situation as x-ray crystallographers are with the water-soluble globular protein. We put the system into a condition in which the high resolution NMR method can be applied. As a result, we can provide a very specific structural prediction that can be tested for relevance under other conditions. In the case of melittin, we think the conformation we find is highly relevant since we have previously published evidence showing that micelle-bound melittin has a conformation very similar to that of melittin bound to a bilayer (Lauterwein et al. 1979. *Biochim. Biophys. Acta.* 556:244–264).

TERWILLIGER: Based on the structure you obtain for the C-terminal region, you should be able to predict between which sets of atoms you should observe a NOE. Do you make any predictions that are not observed?

L. BROWN: In principle, that is correct, except that once you allow internal flexibility, it is difficult to assign a quantitative distance which requires observation of an NOE. However, the calculated structures do not contain any short distances where an NOE might have been expected. If I might extend your question slightly, what you are asking me is whether I have any independent checks of the structure. We have the following results that indicate that micelle-bound melittin has a well-defined conformation. Negative NOE through the polypeptide sequence indicate that no portion of the sequence is highly flexible. Vicinal spin-spin coupling constants $^3J\alpha\beta$ provide additional direct evidence for limited rotational motion about the C^α—C^β bond for Ile-2, Val-I (5 or 8), Thr-II (10 or 11), Ile-17 and Trp-20. Furthermore, the α-CH_2 groups of glycines 1, 3, and 12 as well as the γ-CH_2 and ϵ-CH_2 groups of Lys-I (21 or 23) all give rise to two one-proton resonances in the ^1H NMR spectrum. This indicates limited rotational mobility for the backbone at residues 1, 3, and 12 and for the side chain of Lys-I (21 or 23).

It should also be noted that any experimental data which can be interpreted in terms of bounds to interatomic distances can be used in the distance-geometry algorithm. In terms of NMR parameters, these could include spin-spin coupling constants, aromatic ring current shifts, or line broadening and shifting caused by paramagnetic species. In dealing with temporal averaging, inclusion of other types of data would have the advantage that other forms of dependence on interatomic distances are involved. Alternatively, these other types of data can be checked for consistency with the conformation obtained from NOE data. In the case of melittin 16–24, so far we have measured only a small number of spin-spin coupling constants, but these couplings, as well as the aromatic ring current shifts from the indole ring of Trp-19, are qualitatively consistent with the conformations calculated from the NOE data.

TERWILLIGER: You present evidence that in your micellar system residues 16–24 of melittin are in a generally helical arrangement with the axis of this helix roughly perpendicular to the micellar surface. You then conclude that since both the amino- and carboxyl-termini are near the micelle surface, the central five residues of melittin must form a turn in the micelle interior. As you point out, however, the thickness of the apolar region of this type of micelle is only ~25 Å. The length of a melittin monomer would be ~40 Å if it were a straight α-helix. Considering the relative dimensions of the micelle interior and the melittin molecule, I would like to suggest that a straight α-helix passing through the central region of the micelle would also be consistent with your results.

BROWN: I think it has been said several times here that micelles are highly dynamic systems. Whether the incorporation of a peptide of significant size leaves the micelle shape completely unchanged is not known. One might prefer to think that in these kinds of systems, the peptide is not necessarily conforming to the micelle but rather the micelle, being a highly dynamic structure, is conforming to the peptide. Your question really is, how good is our determination of location using spin labels and could we distinguish between the peptide having a turn or being linear? That is a lower-resolution experiment than the NOE experiment, which shows that the positive charges are distributed radially about the axis of the turn. The spatial resolution of the spin label experiment is described in the caption for Table II. In the interfacial region, radial distances relative to the micelle surface differing in 4–5 Å can be distinguished. Since the positive charges of the lysine and arginine side chains are separated by 10 Å perpendicular to the turn axis, an arrangement of the peptide with the backbone parallel to the surface of the micelle does not appear compatible with our results.

TERWILLIGER: In your paper, you do say that the four positive charges of the C-terminus are radially spread around the helix axis but you do not claim that they are 90° away. In fact, you say that the normal to the plane containing these charges is tilted 0–30° from the helix axis. I think that my model would be a viable explanation of your data within the error of your experiment.

L. BROWN: What you would like me to say at this point is that your amphipathic α-helix is a possibility. I am surprised how similar the results of the two studies are. I have no problem with the two different helical regions in your molecule or with a bend inbetween, but I do see difficulties with how you take your molecule out of the tetramer and put it on the membrane. I would prefer to take this up in your own paper's discussion.

EISENBERG: I would just like to echo what you have said about the similarity between your model and ours, considering that we have used such different techniques. I gather that the precision of your determination of distances from paramagnetic line broadening is better than 10 Å, but poorer than 5 Å.

L. BROWN: You can look at the way we divided the categories of the spin label effects in Table II, where we distinguish from the level of the phosphate out to the methylene of the head group. Outside that would be another category. Inside that for two or three carbon atoms would be a third. Consequently, the resolution of the locations are on the order of 5 Å.

ENGELMAN: You have a redundancy in the information content of the measurement that you point out, the $n \times n$ matrix vs. $3n$ parameters, which means you have $n-3$ independent data sets. Is it possible to check for the internal consistency of a solution by using subsets of your data to see whether you converge to the same solution?

L. BROWN: In fact, we did something like that for another reason. We had difficulties assigning complete spin systems of long side chains like lysine and isoleucine. We saw some α and β proton resonances which had to belong to the carboxyl-terminal portion of the molecule but we did not know to which of the two amino acids. We left them out at the beginning but still obtained similar structures (see text).

MARTIN: Perhaps the previous questions obscure the remarkable advances in the application of NMR spectroscopy to determination of conformation in small proteins that are described in your paper. The application of two-dimensional NMR techniques to reveal juxtaposition of side chains and the distance geometry algorithm are in the forefront of new techniques that promise to be highly useful in determination of conformation.